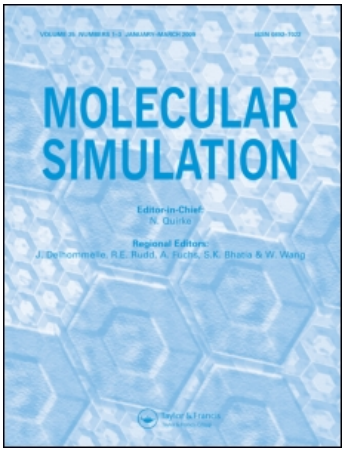

Molecular Simulation
Publication details, including instructions for authors and subscription information:
http://www.informaworld.com/smpp/title~content=t713644482

The molecular basis of the adsorption of bacterial exopolysaccharides on montmorillonite mineral surface

Lina Henao[a]; Karim Mazeau[a]
[a] Centre de Recherches sur les Macromolécules Végétales (CERMAV-CNRS), ICMG FR2607, Joseph Fourier University, Grenoble Cedex 9, France

To cite this Article Henao, Lina and Mazeau, Karim(2008) 'The molecular basis of the adsorption of bacterial exopolysaccharides on montmorillonite mineral surface', Molecular Simulation, 34: 10, 1185 — 1195
To link to this Article: DOI: 10.1080/08927020802235714
URL: http://dx.doi.org/10.1080/08927020802235714

Molecular Simulation
Vol. 34, Nos. 10–15, September–December 2008, 1185–1195

Taylor & Francis
Taylor & Francis Group

The molecular basis of the adsorption of bacterial exopolysaccharides on montmorillonite mineral surface

Lina Henao and Karim Mazeau*

Centre de Recherches sur les Macromolécules Végétales (CERMAV-CNRS), ICMG FR2607, Joseph Fourier University, Grenoble Cedex 9, France

(*Received 11 February 2008; final version received 27 May 2008*)

Rhizospheric exopolysaccharides (EPS) spontaneously aggregate mineral particles. Molecular dynamics simulations with Cerius$^{2®}$ and Materials Studio® programs have been performed to study the adsorption of chemical groups, monosaccharides and oligosaccharides, onto the basal surface of Na-montmorillonite. The estimated enthalpies of adsorption of chemical groups nicely reproduced the expected values. Mono- and oligosaccharides have a preferred geometry of adsorption. Monosaccharides maintained their shape upon adsorption whereas oligosaccharides flattened more or less on the surface, depending on their flexibility. The conformational adaptability was shown to be the leading factor that determined the interaction strength between the EPS and the mineral surface.

Keywords: molecular modelling; clay; polysaccharide; adsorption

1. Introduction

Organic/inorganic hybrid composites are materials that comprise nanometre-size mineral particles dispersed in a polymer matrix. Compared to a pure matrix, these materials exhibit enhanced properties: an increase in the mechanical and thermal performances, and a barrier effect to gas diffusion [1,2]. Most of the matrices considered so far are synthetic polymers; preparing such materials is difficult because of the low compatibility between hydrophobic polymers and the hydrophilic mineral. To overcome this difficulty, the cations located in the interlayer space of the clays are exchanged by tensioactive molecules (principally alkyl ammoniums). The inter layer space thus gains a hydrophobic character and becomes compatible with polymers.

Such hybrid complexes do exist in nature: rhizospheric microorganisms, i.e. living in the vicinity of plant roots, produce exopolysaccharides (EPS). These EPS possess two key properties: they aggregate mineral particles [3] and they can retain a large amount of water [4]. The benefit for bacteria is obvious as they are protected by organo-mineral aggregates against both brutal climatic changes and hydric stress [4–10]. There is also a benefit for the soil, as the presence of aggregates is correlated with soil fertility [11]. Polysaccharides have indeed the additional properties of being biocompatible and biodegradable, two supplementary advantages exploited in an emerging class of biomaterials [12–17].

The macroscopic properties reflect the associations occurring at the molecular scale between polysaccharides, mineral particles and water. The surface of montmorillonite for example, bears negative charges; one may intuitively think that the most favourable organic molecules for adsorption onto such mineral are poly-cations. The situation is apparently more complicated as many rhizospheric EPS are shown to interact with minerals [6,18–24]; they are either neutral or anionic (with one or two charges per repeat unit, generally carboxylic acids). The role of the fine structure of the polysaccharide on its adsorption mechanism onto mineral surfaces remains largely unclear. However, EPS offer a unique opportunity to establish structure–property relationships; their experimental responses to flocculate a colloidal suspension of clays are effectively structure dependant [25,26] and EPS possess a wide variety of structures: they can be linear or branched. When present, the ionisable group is located either on the backbone or on the side chains (Figure 1). To complement the experimental efforts, our objective was thus to reveal, by molecular modelling, the structural factors (if any) of microbial polysaccharides that are responsible for their adsorption on mineral surfaces. Montmorillonite is the chosen mineral; it is widespread on earth, its crystal structure is reported [27] and it is widely studied by molecular modelling (in particular in interactions with organic species) [28–32]. Only the basal surface of montmorillonite was considered in this study as it is statistically the most abundant surface.

2. Material and methods

In this study, we have used the modelling software Cerius$^{2®}$ and Materials Studio® (Accelrys Inc., San

*Corresponding author. Email: karim.mazeau@cermav.cnrs.fr

ISSN 0892-7022 print/ISSN 1029-0435 online

DOI: 10.1080/08927020802235714
http://www.informaworld.com

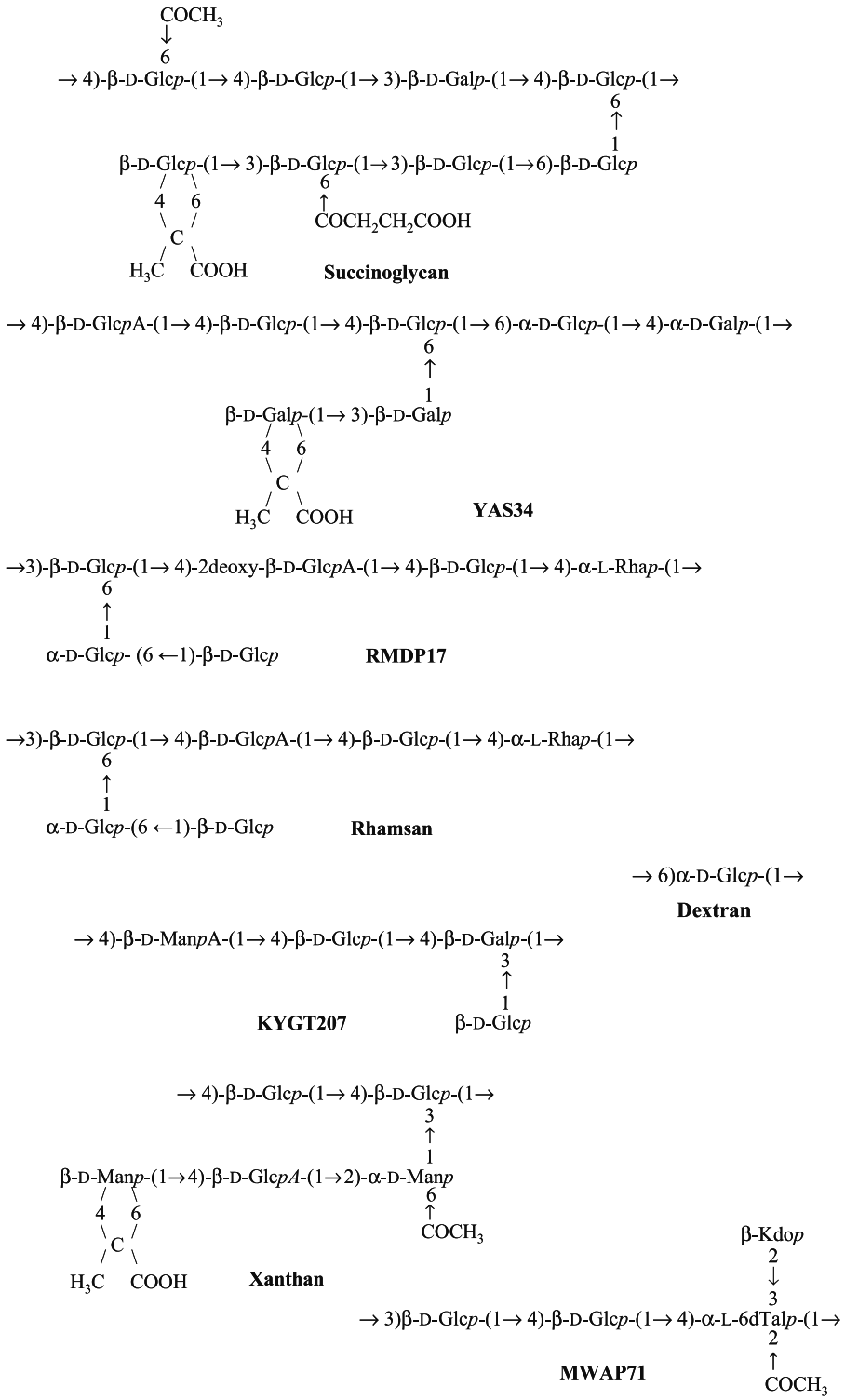

Figure 1. Chemical structures of the polysaccharides considered in this study.

Diego, CA, USA) running on silicon graphics workstations at the Centre d'Expérimentation et de Calcul Intensif, CECIC, Grenoble, France.

3. Construction of the initial structures

3.1 Mineral surface

Montmorillonite is a smectite type mineral clay. It is a hydrophilic mineral that consists of nanometre-thick layers formed by sandwiching an aluminium octahedron sheet between two silicon tetrahedron sheets. The initial unit cell was built from relevant crystallographic coordinates of a pyrophillite crystal, published by Tsipursky and Drits [27], using the crystal builder modulus. The experimental lattice is monoclinic, with space group C2/m, and the lattice parameters: $a = 5.20$, $b = 9.20$, $c = 10.13$ and $\alpha = 90°$, $\beta = 99°$, $\gamma = 90°$. The unit cell is duplicated along the two directions parallel to the sheet planes. Then, we performed substitution of some Al^{3+} by Mg^{2+} in the octahedral layer and substitution of some Si^{+4} atoms by Al^{3+} in the tetrahedral layer in order to obtain the desired final chemical composition of the Wyoming Na-montmorillonite: $Na_{0.75}(Si_{7.75}Al_{0.25})(Al_{3.5}Mg_{0.5})O_{20}(OH)_4$. This structure has a cation exchange capacity (CEC) of 1.01 meq/g; the CEC is defined as the amount of the exchangeable cations retained by the clay to neutralise the negative charge (milliequivalent of positive charge per gram of clay). Periodic boundary conditions are applied in all the three dimensions. Typical a, b dimensions of the periodic cell are 17.8 × 30.4 Å, corresponding to a surface area of 5.4 nm^2. This surface was used to study the adsorption of small molecules (chemical functions and monosaccharides). A larger surface was also built to model the adsorption of the largest structures (oligomers). Cell parameters of the large surface model were 72.8 × 62.1 Å (area of 45 nm^2). The clay mineral is then minimised, equilibrated by molecular dynamics (NPT at 300 K and 1 atm.) and then optimised again. To generate a mineral surface convenient for the simulation, the lattice constant c of the cell was extended to 100 Å. Surfaces were then hydrated by a monolayer of water molecules.

3.2 Organic chemicals

We studied the adsorption of chemical groups, monosaccharides and oligosaccharides; they are all related to the EPS indicated in Figure 1. The chemical groups considered are: methane (CH_4), ethane (CH_3CH_3), methanol (CH_3OH), ethanol (CH_3CH_2OH), 2-propanol ($CH_3CH_2OHCH_3$), methanoic acid (HCOOH), ethanoic acid (CH_3COOH), methanal (HCHO), ethanal (CH_3CHO), dimethyl ketone ($CH_3(CO)CH_3$), methoxymethane (CH_3OCH_3), methyl ethanoate ($CH_3(CO)OCH_3$) and sodium acetate ($CH_3COO^-Na^+$). The twenty monosaccharides considered are indicated in Table 2; the two hydroxyl groups involved in glycosidic bonds have been systematically changed to OMe groups.

The oligomers considered in this part correspond to a unique repeat unit of selected EPS synthetised by rhizospheric microbes: dextran, MWAP71, RMDP17, Rhamsan, xanthan, YAS34 and succinoglycan; their primary structures are reported in Figure 1. A degree of polymerisation of 6 was chosen for the dextran to obtain a molar mass comparable to the other oligomers (Table 4). Polysaccharides are usually highly polydisperses; dextran for example represents a family of homopolysaccharides that feature a substantial number of consecutive α-(1 → 6) linkages in their main chain, usually more than 50% of the total linkages. Dextrans also possess a variable amount of side chains constituted by mono and/or oligosaccharides linked to the main chain by (1 → 3) and (1 → 2) linkages. It is obviously not possible to consider all the possible chemical structures for a given polysaccharide so that each model corresponds only to an idealised structure; consequently, the dextran modelled in our study is only represented by its dominant structural feature (Figure 1). In addition, some of the polysaccharides are known to form multiple helices in solution (xanthan for example); only the simple chain was considered in our study.

Chemical groups, monosaccharides and repeat units of EPS were constructed from standard geometries of bond lengths and bond angles, thanks to the sketcher module. The initial conformation of the pyran ring of monosaccharides is $^4C_1$ for Glc, Man, Gal and Kdo residues or $^1C_4$ for Rha and Tal. In the case of oligosaccharides, values of the conformational parameters describing the relative orientation of two consecutive monomers (torsion angles Φ, Ψ and ω) were derived from the conformational analysis of model disaccharides [33,34]. Torsion angle values correspond to the lowest energy minimum and/or auxiliary minima of the (Φ, Ψ) potential energy surfaces. Explicit hydrogen atoms were used in all model systems. Each structure was then relaxed to minimise energy and avoid atom overlaps.

3.3 Modelling the adsorption

An organic molecule is then inserted in the simulation box above the mineral surface in a random orientation. Configurational sampling was then performed using a combination of energy minimisation and molecular dynamics at elevated temperatures, typically 400–600 K. A typical dynamic simulation lasts 500 ps for the shortest ones, up to 2 ns for the longest ones. Once adsorbed, a 20 Å slab of amorphous water molecules was added to the system. The resulting hydrated model was first minimised, equilibrated for 10 ps and minimised again prior

to analysis. Calculations have been repeated three times on several test cases and the results were consistent.

3.4 Computational details

The Universal force field UFF was used [35]. This choice resulted from a compromise between good accuracy and availability of the parameters for all atom types present in the molecular models. This force field was successfully used in independent studies of organo-clay species [29,36,37]. Furthermore, preliminary tests reveal that this force field correctly reproduces the particular conformational properties of carbohydrates: puckering of the pyran rings and the exo-anomeric effect. The charge equilibration method was used to calculate charges for each atom [38]. Long-range interactions were treated by the Ewald summation technique [39]. The simple point charge model was used for the water molecules.

The minimisation uses the conjugate gradient procedure with the convergence criterion of the root-mean-square of the atomic derivatives of $0.05\,\mathrm{kcal\,mol^{-1}\,\AA^{-1}}$.

Molecular dynamic calculations were based on the canonical NVT ensemble (constant number of particles, volume and temperature). The equations of motion were solved using the standard Verlet algorithm [40], with a time step of 1 fs. The system is coupled to a bath at the desired temperature using Nose's algorithm [41]. During the production molecular dynamics simulations, the positions of the mineral surface atoms were fixed, but all remaining system components (counter ion, organic molecule and water) were allowed to move accordingly.

3.5 Properties

3.5.1 Enthalpies of adsorption

Ten structures (snapshots) were randomly selected and minimised from the molecular dynamic trajectory. The total potential energy of a microstate may be written as:

$$E_{\mathrm{tot}} = E_{\mathrm{clay}} + E_{\mathrm{ligand}} + E_{\mathrm{inter}},$$

where the first three terms represent the energy of the total system, the energy of montmorillonite alone, and the energy of the ligand molecule and consist of both valence and nonbonded components. The last term is the interaction energies between the clay and the ligand (consisting of nonbonded terms only). The enthalpy of adsorption is taken as the negative of the interaction energies of the 10 selected structures:

$$\Delta H_{\mathrm{ads}} = -\langle E_{\mathrm{inter}} \rangle.$$

We were interested by the energy change of the carbohydrate structure when it goes out of the solution to the adsorbed state: ΔE. Dynamic trajectories of the carbohydrate structures were thus performed, in the absence of the mineral surface.

$$\Delta E = E_{\mathrm{ads}} - E_{\mathrm{Free}},$$

where E_{ads} and E_{Free} are the energies of the adsorbed and isolated (in the absence of the mineral surface) conformations, respectively.

3.5.2 Surface area in contact

The estimation of the molecular surface areas was performed with the Connolly dot algorithm [42] with a probe radius of 1.4 Å.

3.5.3 Hydrogen bonds

The method traditionally used to detect a hydrogen bond is geometric: two oxygen atoms are considered hydrogen bonded if the distance between the hydrogen of the donor and the oxygen acceptor is lower than 2.5 Å and if the angle between the oxygen donor, the hydrogen donor and the oxygen acceptor larger than 90°.

4. Results and discussion

A hierarchical approach was chosen to reveal the adsorption behaviour of polysaccharides onto the basal surface of the clay mineral. Adsorption of chemical groups was examined first, followed by adsorption of monosaccharides. Finally, the adsorption of oligosaccharides was considered. Idealised chemical structures of the EPS are given in Figure 1; it was experimentally shown that all of them do adsorb on mineral surfaces. Predicted quantities are the energies associated with the binding and also the geometry of the complexes.

During the dynamics trajectory, the total energy decreases when the saccharide adsorbs onto the surface of the clay mineral, suggesting that the whole modelled system reaches a more stable state. Consequently, the positive values of ΔH_{ads} (or the negative values of E_{int}) indicate that the adsorption is a favorable process.

4.1 Adsorption of functional groups

During the dynamics simulation, the chemical groups explore several adsorption sites of similar energy. Table 1 gives their average interaction energies with the mineral surface. The counter ion has no noticeable effect on the interaction of hydrophobic groups (methyl and ethyl) with the clay surface. In contrast, it strongly participates to the interaction with polar groups. Alcohol and carboxyl groups form hydrogen bonds with the oxygen atoms of the mineral surface; electrostatic interactions (ionic like) also occur, between the oxygen atoms of the organic molecule and the counter ion.

Table 1. Energies (kcal/mol) and interacting areas (Å^2) of several chemical moieties adsorbed onto the mineral surface.

	Without counter ion				With counter ion			
Group	E_c	E_{vw}	E_{tot}	S_{int}	E_c	E_{vw}	E_{tot}	S_{int}
CH_4	0	−6	−6	18	−1	−6	−7	18
CH_3OH	−3	−7	−10	22	−28	−3	−31	24
HCHO	−5	−6	−11	16	−21	−4	−25	23
HCOOH	−1	−7	−8	22	−17	−5	−22	23
CH_3CH_3	0	−9	−9	25	−4	−8	−12	25
CH_3CH_2OH	−2	−11	−13	27	−30	−5	−35	28
CH_3CHO	−5	−10	−15	22	−23	−8	−31	28
CH_3COOH	−1	−11	−12	30	−20	−8	−28	30
CH_3OCH_3	0	−11	−11	34	−31	−6	−37	32
$CH_3CHOHCH_3$	−2	−13	−15	30	−29	−8	−37	30
$CH_3(CO)CH_3$	−2	−13	−15	35	−25	−10	−35	34
$CH_3(CO)OCH_3$	−2	−14	−16	36	−29	−12	−41	41

E_{tot}, total energy; E_c and E_{vw} are its coulomb and Van der Waals components. Standard deviations on energies ranged between 1 and 3 kcal/mol and those on surfaces ranged between 1 and 5 Å^2.

The interaction of very small molecular fragments of saccharides with the mineral surface can be considered unperturbed by structural effects. The interaction is thus optimal and the estimated values of the enthalpies of adsorption give the orders of magnitude of the energies involved upon adsorption. The interaction of the different functions on the mineral surface is globally weak; the energy of a hydrogen bond O—H . . . O and a hydrophobic interaction are typically in the range 4–5 and 1–3 kcal/mol, respectively. Our results are in agreement with these values, suggesting that the force field correctly reproduces the basic interaction energies.

4.2 Monosaccharides and oligosaccharides

The dynamical behaviour of mono- and oligosaccharides differs from that of functional groups. They touched the mineral surface and explored several orientations prior to converging to their preferred adsorption geometry. This suggests that the potential energy surface has many energy minima. The energy decreases gradually with time during the course of the simulation and only the final parts of the trajectories were considered (when the total energy is stabilised to its minimal value), in order to estimate the interaction energies. On average, only 30–40% of the total accessible surface of monosacharides is in direct contact with the mineral surface; this value is remarkably unchanged for the oligomeric fragments.

4.3 Monosaccharides

All the monomers considered in this study are indicated in Table 2 with the structural and energy details of their adsorption on the mineral surface.

The adsorption enthalpy strongly depends on several factors, including the number of pendant groups, their nature, position and orientation with respect to the pyran ring. Figure 2 compares the preferred geometry of interaction of two glucoses 1,6 dimethylated (α and β). Inverting the configuration on the anomeric carbon atom changed the adsorption features of the monosaccharide on the mineral surface.

Here again, the counter ion favours the adsorption of the monosaccharides. The average interaction energy was −30 kcal/mol in the absence of counter ions; it reached −106 kcal/mol in their presence. Inspection of the models reveals the strong similarity of the binding of monosaccharides with that of the functional groups: hydrogen bonds and ionic interactions. Hydrophobic interactions seem to play a particular role. Methyl groups were in direct contact with the surface and the monosaccharide–surface interaction was stronger when more *O*-methoxy groups were present (Table 2).

The group contribution method clearly overestimated the interaction energies. For example, group method predicts an energy of interaction of about −200 kcal/mol for a simple di-substituted glucose molecule. The energies really involved with the adsorption of such molecules are much lower than this expected value, they ranged between −104 and −120 kcal/mol. This is not surprising as the group contribution assumes an optimal interaction whereas, in reality, the adsorption is far from perfect. In addition, structural effects are neglected in the group method; it cannot discriminate between different stereo isomers.

The changes in the conformational energies (ΔE) were minimal for the monosaccharides. They are made of a pyran ring which adopts a dominant chair conformation, except for very rare cases. The chair geometry remained when the monosaccharide is adsorbed, by contrast, side chains showed flexibility.

Table 2. Energetic and geometric characteristics of selected monomers of carbohydrates adsorbed onto the clay mineral surface in the presence or absence of counter ion.

			Without counter ion			With counter ion		
Monomer	Substituents	S_{tot}	E_{int}	S_{int}	ΔE	E_{int}	S_{int}	ΔE
β-D-Glc*p*	Me1	192	−31	69	4	−99	81	13
β-D-Glc*p*	Me1, Me3	205	−35	84	2	−107	93	12
β-D-Glc*p*	Me1, Me4	203	−34	83	7	−104	85	15
β-D-Glc*p*	Me1, Me3, Me4	222	−39	87	6	−111	102	15
β-D-Glc*p*	Me1, Me4, Me6	220	−43	93	8	−123	98	19
β-D-Glc*p*	Me1, Me6	209	−38	83	−3	−113	92	12
α-D-Glc*p*	Me1, Me6	209	−33	76	6	−120	87	17
β-D-Glc*p*	Me1, Me4, 6-$COCH_3$	253	−43	94	1	−110	104	10
β-D-Glc*p*	Me1, Me3, 6-$COCH_2$ CH_2COOH	307	−48	116	13	−146	129	26
β-D-Glc*p*A	Me1, Me4	208	−34	82	−3	−88	82	6
2deoxy-β-D-Glc*p*A	Me1, Me4	199	−36	83	−2	−95	93	19
β-D-Glc*p*	Me1, 4-6pyruvate	239	−35	86	0	−84	84	4
β-D-Gal*p*	Me 1, Me 3	209	−35	79	3	−94	81	7
α-D-Gal*p*	Me 1, Me 4	202	−32	68	−3	−90	77	12
β-D-Gal*p*	Me 1, 4-6pyruvate	235	−31	81	8	−97	90	15
α-D-Man*p*	Me 1, Me 2, 6$COCH_3$	241	−36	82	5	−95	96	17
β-D-Man*p*	Me 1, 4-6pyruvate	235	−31	81	−1	−92	91	2
α-L-Rha*p*	Me 1, Me 4	193	−25	58	1	−53	62	3
β-Kdo*p*	Me2	225	−30	72	4	−106	77	14
α-L-6dTal*p*	Me1, Me3, Me4, 2$COCH_3$	242	−24	58	4	−92	74	14

Note: Kdo is the 3-deoxy-D-Manno-oct-2-ulosonic acid. Energy of interaction (E_{int} in kcal/mol); difference in energy between the free state and the adsorbed state (ΔE in kcal/mol). Total solvent exposed surface (S_{tot} in $Å^2$), surface in interaction (S_{int} in $Å^2$). Standard deviations on energies ranged between 2 and 8 kcal/mol and those on surfaces ranged between 1 and 14 $Å^2$.

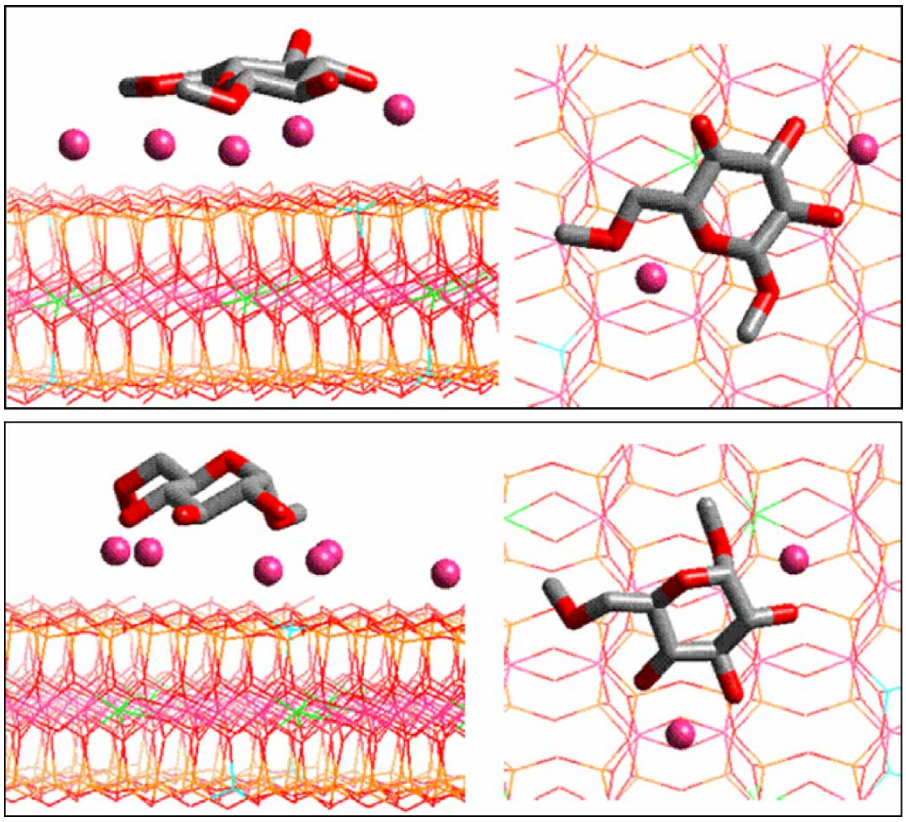

Figure 2. Equilibrium adsorbed geometry of β-glucose (top) and α-glucose (bottom) methylated at positions 1 and 6. Left side views, right front views. Hydrogen atoms are omitted for clarity.

4.4 Oligomers: repeat units of EPS

Given the results of the previous section, simulations on the oligomeric structures of carbohydrates were systematically performed in the presence of the counter ions. Their energies of interaction with the clay surface are given in Table 3, the geometrical aspects of the adsorption are given in Table 4.

Inspecting the molecular models shows that the monomers in the adsorbed conformational state do not systematically adopt the unperturbed orientation revealed in the preceding section. To illustrate this, Figure 3 gives the adsorbed fragment of dextran; among its six α-Glc residues; four of them adsorb in an identical geometry already observed in the study of free monosaccharides; by contrast, the remaining two α-Glc behave differently. Chemical connectivity induces geometrical constraints that limit the number of accessible orientations of the constituent monosaccharides with respect to the mineral surface. However, the potential energy surface contains a huge amount of energy minima; monomer units that are part of a polymer simply explore secondary potential wells.

The presence of the surface systematically induced an increase of the internal energy of the EPS fragments. The conformation was thus less stable when adsorbed than when isolated; the difference reaches 20% in the case of RMDP17 and succinoglycan. The presence of the surface also induced an increase of the total accessible surface of the organic molecule. The oligosaccharides unfolded and thus maximised the contact area with the mineral surface. Figures 3 and 4 show the repeat units of MWAP71 and RMDP17 adsorbed on the surface. The RMDP17 oligosaccharide flattened on the surface, all the monomer units were in direct contact with the surface (Figure 4). On the other hand, the pendent monomer Kdo (which bears the carboxylic group) of MWAP71 was not in contact with the clay. Root mean square deviation (RMSD) compares coordinates of the conformation when adsorbed with the free conformation; it indicates the extent of modification of the shape of the sugar with adsorption. RMSD strongly vary from one EPS to the other; it reached 17% for succinoglycan and it was minimal for the MWAP71 and YAS34.

Table 3. Selected characteristics of the repeat units of EPS.

	ΔH_{Ads}	E_{adsorb}	E_{Free}	RMSD
Dextran	351	725	646	0.0234
KYGT207	240	486	442	0.0304
MWAP71	151	421	394	0.0145
Rhamsan	333	686	615	0.0362
RMDP17	316	603	509	0.0465
Succinoglycan	564	950	785	0.0245
Xanthan	268	592	541	0.0230
YAS34	445	958	841	0.0153

ΔH_{Ads}, enthalpy of adsorption of the oligomer on the mineral surface; E_{adsorb}, average energy of the adsorbed conformation; E_{Free}, average energy of the equilibrium conformation in the absence of the surface; RMSD, root mean square deviation per atom between the free and the adsorbed conformations. Energies are given in kcal/mol.

Table 4. Geometric characteristics (in Å^2) of the adsorption of the repeat units of EPS.

	$S_{totcompl}$	S_{Free}	$S_{interact}$	Mw
Dextran	806	743	345	1018
KYGT207	550	531	239	708
MWAP71	599	595	202	778
Rhamsan	796	737	340	1016
RMDP17	802	745	314	1000
succinoglycan	1244	1071	549	1554
Xanthan	773	735	304	982
YAS34	942	967	386	1264

$S_{totcompl}$, solvent accessible surface of the adsorbed conformation; S_{Free}, solvent accessible surface of the free conformation; $S_{interact}$, area in interaction. Molecular masses of the different fragments of EPS are also indicated (Mw).

Figure 5 gives the correlation between the estimated enthalpies of adsorption and the effective interacting area. The linear relationship suggests that the real area in interaction is the critical factor on which depends the adsorption of the tested EPS. Structural factors play a role in the deviation with respect to the master line.

All these results strongly suggest that the oligosaccharide have one (or several) unperturbed solution conformation and another conformation when it is adsorbed on a surface. In contrast with the rigid monosaccharides, the glycosidic bonds linking the monomers together provide conformational freedom in an oligomeric structure. Such flexibility allows the oligomer to change its shape upon interaction with the mineral surface. In other words, the more flexible the structure, the stronger the interaction. It is thus obvious that the deformation ability (to optimise the interaction) of linear polymers is larger than that of branched polymers for which the side chains induce a steric hindrance that restrict the flexibility of the whole molecule. Accordingly, the fragment of MWAP71 (Figure 4) is rigid; its conformational adaptation is restricted to 3 glycosidic bonds and the Kdo pendant group is not in interaction with the surface. In contrast, the large flexibility of RMDP17 (five glycosidic bonds) allows all its monomer units being in contact with the surface.

4.5 Comparison with the experiments

The accuracy of the models could be assessed by comparing the predicted data to the experimental data. Our results revealed the strong participation of the counter ion in the stability of the complex. They considerably increased the interaction energy between the EPS segment and the mineral surface. The crucial role of electrostatic (ionic) interactions through counter ions

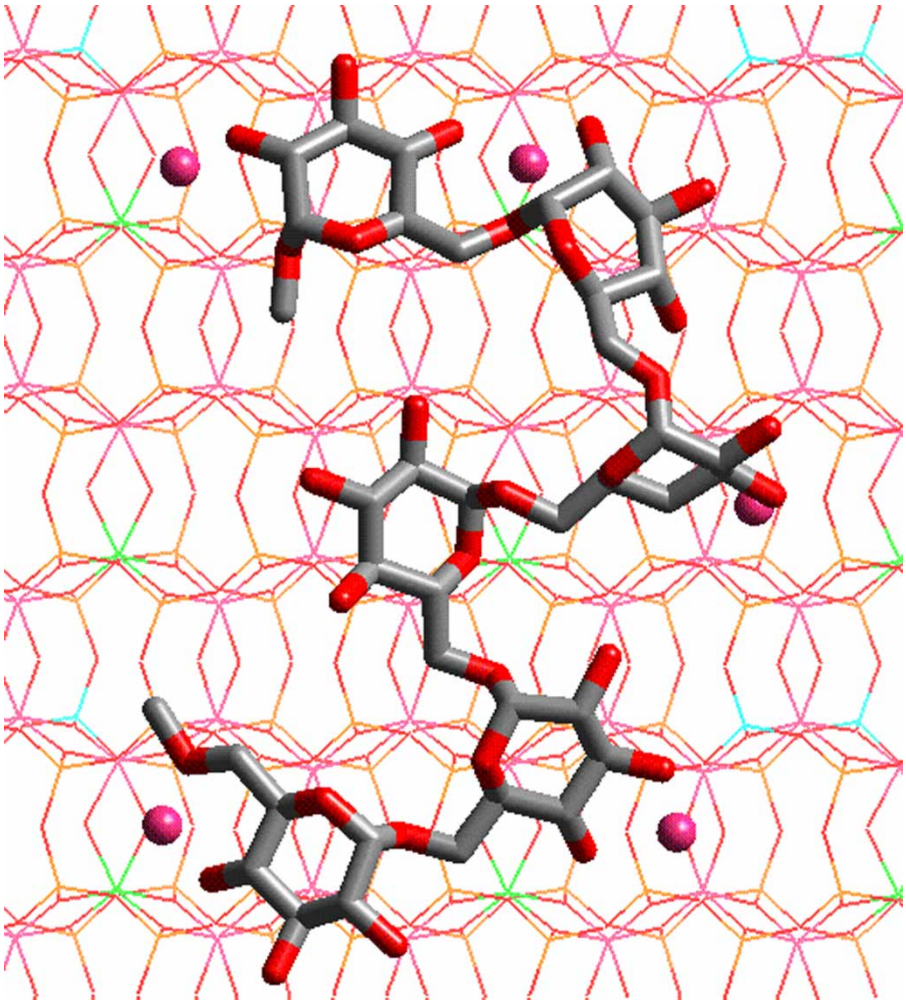

Figure 3. Equilibrium adsorbed geometry of the dextran fragment. Hydrogen atoms and water molecules are omitted for clarity.

is also revealed by many experiments [22,43–45]. Complexes were also stabilised by hydrogen bonds and hydrophobic interactions. Experimental data show that adsorption of ethyl(hydroxyethyl)cellulose on talc is destabilised by urea, which is an hydrogen bond breaker [12]. Finally, the importance of the hydrophobic interactions is counter intuitive; it is however consistent with NMR results which indicate that aliphatic chains are in direct contact with montmorillonite [46]. Our models also showed that the oligosaccharides undergo conformational changes between the solution states and the adsorbed state. Quartz crystal microbalance with dissipation monitoring (QCM-D) experiments reveal that the adsorbed conformation of dextran on alumina differs from that in solution [47].

Experiments are also performed to establish the structure–property relationships. The ability of several EPS to flocculate a colloidal suspension of clay particles is compared [26]. Experiments measure the average size of the flocs which indirectly reflects the efficiency of the EPS to bridge different mineral particles. Such measurements thus give an indication of the affinity of the EPS with the mineral surface. An interaction efficiency coefficient (IEC) was defined in order to allow the comparison between the experimental and modelling approaches. The IEC corresponded to the enthalpy of adsorption, normalised by the effective interaction area. Experimental floc size in the presence of succinoglycan (335 μm) is much larger than that of xanthan (158 μm); even though the molar mass of the xanthan sample is twice the mass of succinoglycan. In qualitative agreement with the experiments, IEC of succinoglycan (1027 cal/mol$Å^2$) was estimated larger than that of xanthan (882 cal/mol$Å^2$). The molecular masses of dextran and YAS34 are identical (2×10^6 g mol^{-1}), their floc sizes are 140 and 213 μm, respectively. YAS34 is thus much more efficient than dextran with respect to flocculation ability. Estimated IEC reproduced the experimental tendency: they were estimated at 1017 and 1152 cal/mol$Å^2$ for dextran and YAS34, respectively.

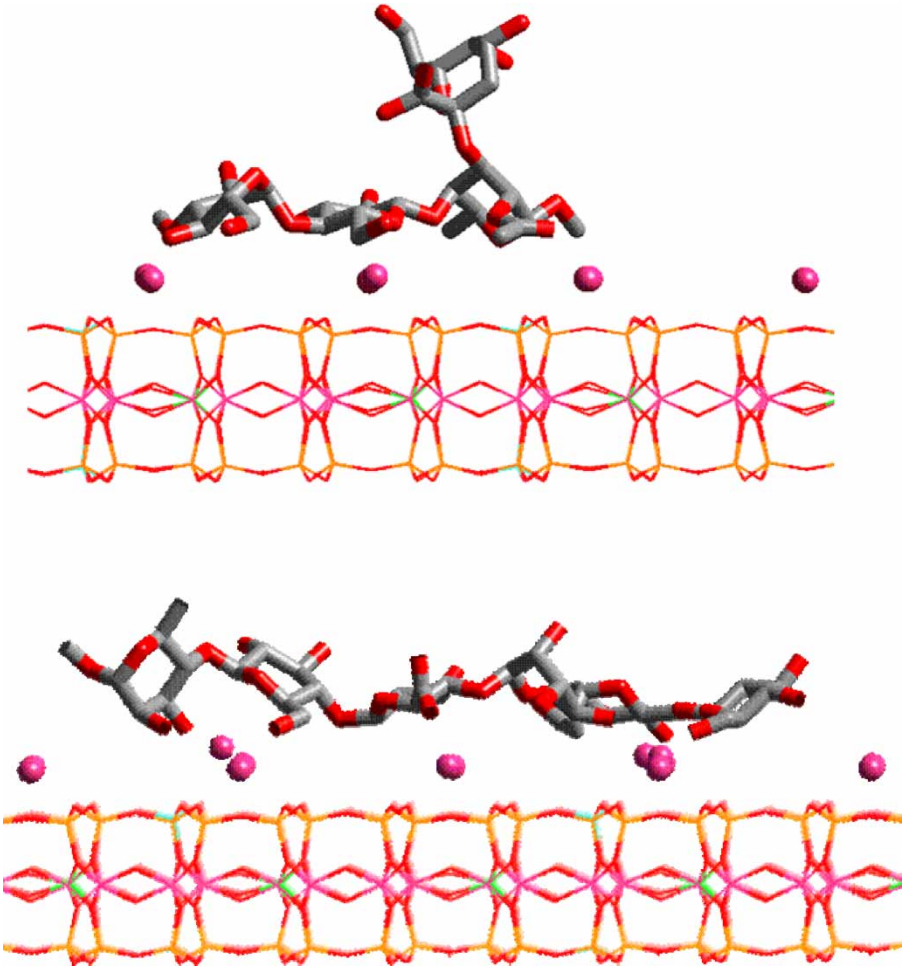

Figure 4. Equilibrium adsorbed geometry of the MWAP71 (top) and the RMDP17 (bottom). Hydrogen atoms and water molecules are omitted for clarity.

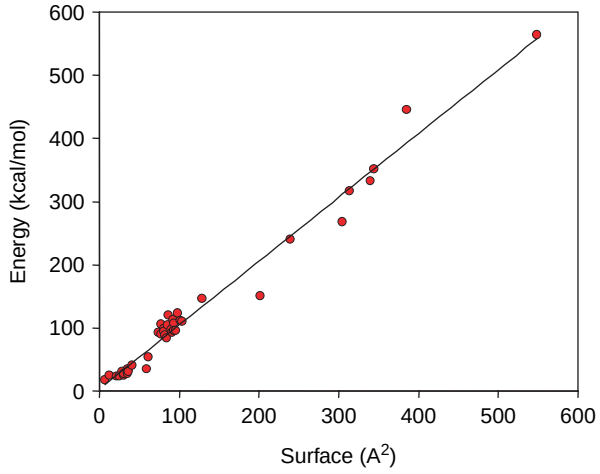

Figure 5. Energy of adsorption as a function of the interacting area.

Quantitative comparison between experimental data and the present modelling results is not possible because of both experimental difficulties and assumptions in modelling. Molar masses of the different polysaccharides studied experimentally differ by almost a factor of 20; it is well recognised that such characteristics strongly impact on polymer adsorption on surfaces. In addition, modelling is performed on idealised chemical structures of the EPS and the analysis of the results was based only on the enthalpies of adsorption. The free energy of adsorption would be the choice parameter but the entropic contribution is hardly accessible. The entropy depends on two major contributions: de-solvation of the surfaces, which is a favourable process, and the conformational restrictions of the polymer upon adsorption; which gives non-favourable entropy.

5. Conclusion

Atomic level molecular simulations were applied to investigate the interaction features of model molecules mimicking bacterial EPS (in their neutral forms) with the basal surface of Na-montmorillonite surface. The study has been performed using Cerius[2] and Materials Studio modelling programs.

It was found that hydrogen bonds, electrostatic and hydrophobic interactions are present in the model systems and provide a significant effect on the adsorption strength of EPS fragments on the mineral surface. The adsorption of monosaccharides was dependant on the nature of the monomer and its side chains. The six-membered ring stayed in its preferred geometry when adsorbed. In contrast, oligosaccharides changed their shape upon adsorption. It was found that the enthalpies of adsorption linearly increase with increasing the interacting surface area, suggesting that the key factor determining the adsorption is the ability of the EPS to unfold in order to maximise its surface in contact. The most flexible structures were the most favourable candidates for adsorption. The present modelling was able to predict a complex physical adsorption phenomenon in agreement with the experimental results.

References

[1] S.S. Ray and M. Okamoto, *Polymer/layered silicate nanocomposites: a review from preparation to processing*, Prog. Polym. Sci. 28 (2003), pp. 1539–1641.

[2] M. Alexandre and P. Dubois, *Polymer-layered silicate nanocomposites: preparation, properties and uses of a new class of materials*, Mater. Sci. Eng. R: Rep. R28 (2000), pp. 1–63.

[3] J.M. Dorioz, M. Robert, and C. Chenu, *The role of roots, fungi and bacteria on clay particle organization. An experimental approach*, Geoderma 56 (1993), pp. 179–194.

[4] C. Chenu, *Clay- or sand-polysaccharide associations as models for the interface between microorganisms and soil: water related properties and microstructure*, Geoderma 56 (1993), pp. 143–156.

[5] E.B. Roberson and M.K. Firestone, *Relationship between desiccation and exopolysaccharide production in a soil* Pseudomonas *sp*. Appl. Environ. Microbiol. 58 (1992), pp. 1284–1291.

[6] Y. Alami, W. Achouak, C. Marol, and T. Heulin, *Rhizosphere soil aggregation and plant growth promotion of sunflowers by an exopolysaccharide-producing* Rhizobium *sp. strain isolated from sunflower roots*, Appl. Environ. Microbiol. 66 (2000), pp. 3393–3398.

[7] M. Ashraf, S. Hasnain, O. Berge, and T. Mahmood, *Inoculating wheat seedlings with exopolysaccharide-producing bacteria restricts sodium uptake and stimulates plant growth under salt stress*, Biol. Fertil. Soils 40 (2004), pp. 157–162.

[8] P.G. Hartel and M. Alexander, *Role of extracellular polysaccharide production and clays in the desiccation tolerance of cowpea bradyrhizobia*, Soil Sci. Soc. Am. J. 50 (1986), pp. 1193–1198.

[9] C. Chenu, Y. Le Bissonnais, and D. Arrouays, *Organic matter influence on clay wettability and soil aggregate stability*, Soil Sci. Soc. Am. J. 64 (2000), pp. 1479–1486.

[10] D. Cosentino, C. Chenu, and Y. Le Bissonnais, *Aggregate stability and microbial community dynamics under drying–wetting cycles in a silt loam soil*, Soil Biol. Biochem. 38 (2006), pp. 2053–2062.

[11] C. Chenu, J. Guerif, and A.M. Jaunet, *Polymer bridging: A mechanism of clay and soil structure stabilization by polysaccharides*, Transactions, World Congress of Soil Science, 15th, Acapulco, Mexico, July 10–16, 3a (1994), pp. 403–410.

[12] S. Simon, D. Le Cerf, L. Picton, and G. Muller, *Adsorption of cellulose derivatives onto montmorillonite: A SEC-MALLS study of molar masses influence*, Colloids Surf A: Physicochem. Eng. Aspects 203 (2002), pp. 77–86.

[13] H.-M. Park, M. Misra, L.T. Drzal, and A.K. Mohanty, \"*Green*\" *Nanocomposites from cellulose acetate bioplastic and clay: Effect of eco-friendly triethyl citrate plasticizer*, Biomacromolecules 5 (2004), pp. 2281–2288.

[14] H.-M. Park, A.K. Mohanty, L.T. Drzal, E. Lee, D.F. Mielewski, and M. Misra, *Effect of sequential mixing and compounding conditions on cellulose acetate/layered silicate nanocomposites*, J. Polym. Environ. 14 (2006), pp. 27–35.

[15] S.F. Wang, L. Shen, Y.J. Tong, L. Chen, I.Y. Phang, P.Q. Lim, and T.X. Liu, *Biopolymer chitosan/montmorillonite nanocomposites: Preparation and characterization*, Polym. Degrad. Stab. 90 (2005), pp. 123–131.

[16] M. Darder, M. Colilla, and E. Ruiz-Hitzky, *Biopolymer-clay nanocomposites based on chitosan intercalated in montmorillonite*, Chem. Mater. 15 (2003), pp. 3774–3780.

[17] M. Darder, M. Colilla, and E. Ruiz-Hitzky, *Chitosan-clay nanocomposites: Application as electrochemical sensors*, Appl. Clay Sci. 28 (2005), pp. 199–208.

[18] J. Labille, F. Thomas, I. Bihannic, and C. Santaella, *Destabilization of montmorillonite suspensions by* Ca^{2+} *and succinoglycan*, Clay Miner. 38 (2003), pp. 173–185.

[19] N. Amellal, G. Burtin, F. Bartoli, and T. Heulin, *Colonization of wheat roots by an exopolysaccharide-producing Pantoea agglomerans strain and its effect on rhizosphere soil aggregation*, Appl. Environ. Microbiol. 64 (1998), pp. 3740–3747.

[20] C. Chenu and J. Guerif, *Mechanical strength of clay minerals as influenced by an adsorbed polysaccharide*, Soil Sci. Soc. Am. J. 55 (1991), pp. 1076–1080.

[21] C. Chenu, *Influence of a fungal polysaccharide, scleroglucan, on clay microstructures*, Soil Biol. Biochem. 21 (1989), pp. 299–305.

[22] K.M. Dontsova and J.M. Bigham, *Anionic polysaccharide sorption by clay minerals*, Soil Sci. Soc. Am. J. 69 (2005), pp. 1026–1035.

[23] M. He and Y. Horikawa, *Partial deflocculation of mutual flocs of allophane and halloysite by xanthan and chitosan and relevance to particle arrangement in the flocs*, Soil Sci. Plant Nutr. (Tokyo) 46 (2000), pp. 81–87.

[24] S.M. Rao, A. Sridharan, and M.R. Shenoy, *Influence of starch polysaccharide on the remolded properties of two Indian clay samples*, Can. Geotech. J. 30 (1993), pp. 550–553.

[25] A. Olness and C.E. Clapp, *Occurrence of collapsed and expanded crystals in montmorillonite–dextran complexes*, Clays and Clay Miner. Proc. Conf. 21 (1973), pp. 289–293.

[26] J. Labille, F. Thomas, M. Milas, and C. Vanhaverbeke, *Flocculation of colloidal clay by bacterial polysaccharides: Effect of macromolecule charge and structure*, J. Colloid Interface Sci. 284 (2005), pp. 149–156.

[27] S.I. Tsipursky and V.A. Drits, *The distribution of octahedral cations in the 2:1 layers of dioctahedral smectites studied by oblique-texture electron diffraction*, Clay Miner. 19 (1984), pp. 177–193.

[28] P. Capkova, M. Pospisil, M. Valaskova, D. Merinska, M. Trchova, Z. Sedlakova, Z. Weiss, and J. Simonik, *Structure of montmorillonite cointercalated with stearic acid and octadecylamine: Modeling, diffraction, IR spectroscopy*, J. Colloid Interface Sci. 300 (2006), pp. 264–269.

[29] A. Gaudel-Siri, P. Brocorens, D. Siri, F. Gardebien, J.-L. Bredas, and R. Lazzaroni, *Molecular dynamics study of e-caprolactone intercalated in wyoming sodium montmorillonite*, Langmuir 19 (2003), pp. 8287–8291.

[30] P. Capkova, P. Maly, M. Pospisil, Z. Klika, H. Weissmannova, and Z. Weiss, *Effect of surface and interlayer structure on the fluorescence of rhodamine B-montmorillonite: Modeling and experiment*, J. Colloid Interface Sci. 277 (2004), pp. 128–137.

[31] M. Fermeglia, M. Ferrone, and S. Pricl, *Computer simulation of nylon-6/organoclay nanocomposites: Prediction of the binding energy*, Fluid Phase Equilib. 212 (2003), pp. 315–329.

[32] P. Capkova, J.V. Burda, Z. Weiss, and H. Schenk, *Modeling of aniline-vermiculite and tetramethylammonium-vermiculite; test of force fields*, J. Mol. Model. 5 (1999), pp. 8–16.

[33] S. Perez, M. Kouwijzer, K. Mazeau, and S.B. Engelsen, *Modeling polysaccharides: Present status and challenges*, J. Mol. Graph. 14 (1996), pp. 307–321.

[34] C. Vanhaverbeke, A. Heyraud, and K. Mazeau, *Conformational analysis of the exopolysaccharide from Burkholderia caribensis strain MWAP71: Impact on the interaction with soils*, Biopolymers 69 (2003), pp. 480–497.

[35] A.K. Rappe, C.J. Casewit, K.S. Colwell, W.A. Goddard, III, and W.M. Skiff, *UFF, a full periodic table force field for molecular mechanics and molecular dynamics simulations*, J. Am. Chem. Soc. 114 (1992), pp. 10024–10035.

[36] R. Toth, A. Coslanich, M. Ferrone, M. Fermeglia, S. Pricl, S. Miertus, and E. Chiellini, *Computer simulation of polypropylene/organoclay*

nanocomposites: Characterization of atomic scale structure and prediction of binding energy, Polymer 45 (2004), pp. 8075–8083.
[37] F. Gardebien, J.-L. Bredas, and R. Lazzaroni, *Molecular dynamics simulations of nanocomposites based on poly (e-caprolactone) grafted on montmorillonite clay*, J. Phys. Chem. B 109 (2005), pp. 12287–12296.
[38] A.K. Rappe and W.A. Goddard, III, *Charge equilibration for molecular dynamics simulations*, J. Phys. Chem. 95 (1991), pp. 3358–3363.
[39] H.Q. Ding, N. Karasawa, and W.A. Goddard, III, *Atomic level simulations on a million particles: The cell-multipole method for Coulomb and London nonbond interactions*, J. Chem. Phys. 97 (1992), pp. 4309–4315.
[40] L. Verlet, *Computer "experiments" on classical fluids. I. Thermodynamical properties of Lennard-Jones molecules*, Phys. Rev. 159 (1967), pp. 98–103.
[41] D.J. Evans and B.L. Holian, *The Nose–Hoover thermostat*, J. Chem. Phys. 83 (1985), pp. 4069–4074.
[42] M.L. Connolly, *Computation of molecular volume*, J. Am. Chem. Soc. 107 (1985), pp. 1118–1124.
[43] L.G. Fuller, T.B. Goh, D.W. Oscarson, and C.G. Biliaderis, *Flocculation and coagulation of Ca- and Mg-saturated montmorillonite in the presence of a neutral polysaccharide*, Clays Clay Miner. 43 (1995), pp. 533–539.
[44] Y.M. Kanaani, A. Adin, and C. Rav-Acha, *Biofilm interactions in water reuse systems: Adsorption of polysaccharide to kaolin*, Water Sci. Technol. 26 (1992), pp. 673–682.
[45] B. Gu and H.E. Doner, *The interaction of polysaccharides with Silver Hill illite*, Clays Clay Miner. 40 (1992), pp. 151–156.
[46] A.J. Simpson, M.J. Simpson, W.L. Kingery, B.A. Lefebvre, A. Moser, A.J. Williams, M. Kvasha, and B.P. Kelleher, *The application of 1H high-resolution magic-angle spinning NMR for the study of clay-organic associations in natural and synthetic complexes*, Langmuir 22 (2006), pp. 4498–4503.
[47] K.D. Kwon, H. Green, P. Bjoeoern, and J.D. Kubicki, *Model bacterial extracellular polysaccharide adsorption onto silica and alumina: Quartz crystal microbalance with dissipation monitoring of dextran adsorption*, Environ. Sci. Technol. 40 (2006), pp. 7739–7744.